Electromagnetic-Circuital-Thermal Multiphysics Simulation Method: A Review

**Huan Huan Zhang[1, *], Pan Pan Wang[1], Shuai Zhang[1], Long Li[1, *],
Ping Li[2], Wei E. I. Sha[3], and Li Jun Jiang[4]**

(*Invited*)

Abstract—Electromagnetic-circuital-thermal multiphysics simulation is a very important topic in the field of integrated circuits (ICs), microwave circuits, antennas, etc. This paper presents a comprehensive review of the state of the art of electromagnetic-circuital-thermal multiphysics simulation method. Most efforts were focused on electromagnetic-circuital co-simulation and electromagnetic-thermal co-simulation. A brief introduction of related theories like governing equations, numerical methods, and coupling mechanisms is also included.

1. INTRODUCTION

With the continuous improvement of the technological level of integrated circuits (ICs), the operating frequency and integration density are becoming higher and higher, which brings huge challenges to the simulation of integrated circuits. On one hand, the wave effect becomes noticeable as the working frequency increases. For instance, the electromagnetic coupling between the interconnects and package will lead to the signal integrity problem. In this situation, the simulation accuracy cannot be guaranteed if only the classical circuit theory is adopted. Therefore, full-wave electromagnetic simulation method must be included to implement electromagnetic-circuital co-simulation. On the other hand, high integration level will not only raise the density of the devices and interconnects, but also increase the power density, resulting in difficulties in thermal management. Moreover, if the temperature of ICs increases greatly, it will cause the change of material properties like permittivity, conductivity, etc., which will have an influence on the functions of ICs. As a result, the mutual effects between EM and thermal must also be taken into account. To sum up, the electromagnetic-circuital-thermal multiphysics simulation becomes necessary and significant in the design of ICs. Actually, such kinds of modeling and simulation requirements are also very common in the field of microwave circuits and antennas.

Currently, there are plenty of literatures related to electromagnetic-circuital co-simulation method (or called hybrid field and circuit simulation method) and the electromagnetic-thermal co-simulation method. So in Sections 2.1 and 2.2 of this paper, we will take a general review of the state-of-the-art. Then we will give a brief introduction of the simulation method for the electromagnetic-circuital-thermal multiphysics design in Section 3. Conclusions are drawn in Section 4.

2. OVERVIEW OF THE STATE-OF-THE-ART

2.1. Electromagnetic-Circuital Co-Simulation Method

In most electromagnetic-circuital co-simulation method, the whole system is mainly divided into two parts: electromagnetic structures and lumped circuits. Full-wave method including finite-difference time-domain (FDTD) method [1], finite element method (FEM) [2], and method of moments (MoM) [3] are adopted to simulate the electromagnetic structures like interconnects and package. The lumped circuits are analyzed by circuit theory. Finally, the interface between the electromagnetic part and circuit part is built to couple them together. There are two kinds of electromagnetic-circuital co-simulation methods. One is the frequency domain method, namely harmonic balance method [4, 5], and the other is the time domain method [8–37]. Since the time domain method is more suitable for the nonlinear, wideband, and multiphysics problem, it captures lots of attention in recent years. In the following, we will introduce the selection of time-domain full-wave method and the analysis method of lumped circuits, respectively.

1) The selection of time-domain full-wave method

The finite-difference time-domain method, finite-element time-domain (FETD) method [6, 7], and time-domain integral equation (TDIE) [8–11] method are three mainstream time-domain full-wave methods in computational electromagnetics. Due to its simplicity, the FDTD method was applied to electromagnetic-circuital co-simulation initially [12–17]. The global time-domain analysis of microwave circuits involving highly nonlinear phenomena such as injection locking and intermodulation, along with parasitic effects, and electromagnetic compatibility (EMC) issues are studied in [16]. For circuits providing complex functionality, two-port or possibly multiport devices, whether passive or active, are sure to appear in the circuits. Therefore, an efficient scheme for processing arbitrary multiport devices is investigated in [17]. However, the classical FDTD method requires orthogonal grids, resulting in the staircasing effects. A high mesh density is required to model structures with curved surfaces. Tetrahedron elements and high-order discretization schemes can be used in the FETD method. Thus, it usually has a higher modeling accuracy. The FETD method was widely adopted in electromagnetic-circuital co-simulation [18–20]. An extension of the unconditionally stable FETD method for the global electromagnetic analysis of active microwave circuits is proposed in [18]. Co-simulation of the linear network and nonlinear circuits in an integrated circuit system is realized in [19]. The proposed algorithm extends the capability of the existing field-circuit solver to model more complex and mixed-scale hybrid circuits. Incorporating multiport lumped networks in terms of admittance matrices into a hybrid field-circuit solver is investigated in [20]. Besides the time-domain differential equation method, the TDIE method was also applied to electromagnetic-circuital co-simulation [21–27]. In [24], the nonlinear equivalent circuit equation is coupled into the time-domain surface and volume electric field integral equations to form a field-circuit system equation. Then, this nonlinear system matrix equation is directly solved by the Newton-Raphson method. However, for a large and complicated microwave nonlinear circuit, the time consumption of the Newton iteration process is often unacceptable in this conventional method. Consequently, in [25], the improved solution scheme is proposed to improve the calculation efficiency of the process of the Newton iteration. In [26], a field-circuit coupling method is presented for the analysis of microwave circuit included with nonlinear physical model-based semiconductor devices. However, the TDIE method is not good at analyzing highly inhomogeneous object. For real-world problems, the electromagnetic structure usually includes complex dielectric substrates, vias, solder balls, microstrip lines, etc., which is difficult to be handled by the TDIE method. Consequently, it is not widely used in electromagnetic-circuital co-simulation.

In summary, the FETD method is preferred for electromagnetic-circuital co-simulation. However, a large global matrix equation has to be solved for each time step in the FETD method, resulting in a great amount of computational cost. The discontinuous Galerkin time domain (DGTD) method [28–32], as a differential equation method, has attracted great attention in recent years. It supports an element-level domain decomposition, avoiding the solution to a large sparse matrix equation. Moreover, the DGTD method is easy to be parallelized, thus suitable for modeling large-scale problem with parallel computing technique. Additionally, the coupled EM-circuit equation is only related to the elements connected with the circuit network. So only a small nonlinear equation needs to be solved at each time step when nonlinear component is included in the lumped circuits.

2) The analysis method of lumped circuits

Firstly, we can divide the lumped circuits into four types, including linear circuits with known internal details (Type A), nonlinear circuits with known internal details (Type B), linear circuits with unknown internal details (Type C), and nonlinear circuits with unknown internal details (Type D). Fig. 1 illustrates the circuits with known and unknown internal details connected with the electromagnetic structure. Here, the internal details refer to the network topology and component information of the original circuit or equivalent circuit. Linear circuits usually consist of resistors, capacitors, and inductors, while nonlinear circuits are usually composed of diodes, transistors, etc.
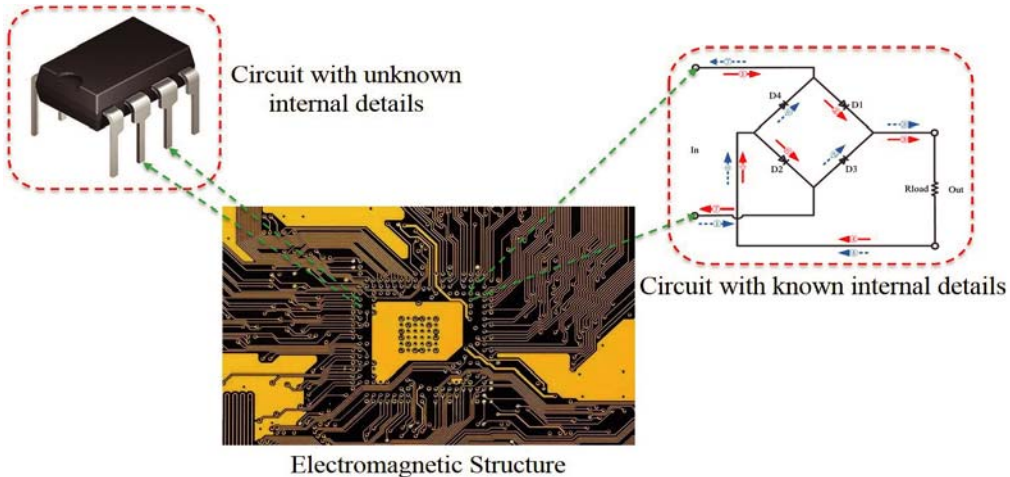

Figure 1. Different circuit types of electromagnetic and circuital co-simulation.

The modified nodal analysis method [33] can be used to construct circuit equations for the lumped circuits with known internal details (both Type A and Type B). It is worth mentioning that the nonlinear equations will be formed for the nonlinear circuits. The solution methods for nonlinear equations like Newton-Raphson algorithm are needed in this case [34]. Many scholars have studied the electromagnetic-circuital co-simulation problem when the internal details of the circuits are known. The major difference among their works lies in the time-domain full-wave simulation adopted. All the aforementioned CEM methods including FDTD [16], FETD [18, 19], TDIE [21, 22], and DGTD [35, 36] have been used for the electromagnetic-circuital co-simulation. As an example, Fig. 2 shows the electromagnetic-circuital co-simulation of a MESFET microwave power amplifier. Port 1 and port 4 of the matching network are connected with linear circuits, while port 2 and port 3 are connected with nonlinear circuits.

In real applications, the circuit details are not always available due to the intellectual property (IP) protection. Thus, the circuit equations cannot be obtained by classical circuit theory. For linear circuits with unknown internal details (Type C), they can be considered as black boxes characterized by scattering or admittance matrices. The scattering matrices can be converted into admittance matrices using the microwave network theory. The admittance matrices in the Laplace domain can be transformed into the time domain. Thus, the time-domain I-V relation of the lumped network is obtained, which can be coupled with the field equations to complete the electromagnetic-circuital co-simulation. FDTD [17], FETD [20], and DGTD [37] methods have been used to solve this kind of problems. Fig. 3 illustrates an example of this case.

We can only find a handful of works on the electromagnetic-circuital co-simulation problem with Type D circuits, whose features are described by behavioral macromodels in existing works. For instance, the IBIS model is integrated with the transmission-line modeling method in [38]. However, the accuracy of the IBIS model is not enough for recent technologies with higher data communication speed and more sophisticated devices. In [39], the Gaussian radial basis function (RBF) behavioral model is coupled with the FDTD method. Actually, the sigmoidal basis function (SBF) behavioral model can give more accurate results with fewer basis functions than RBF model [40]. So recently the TDIE and DGTD
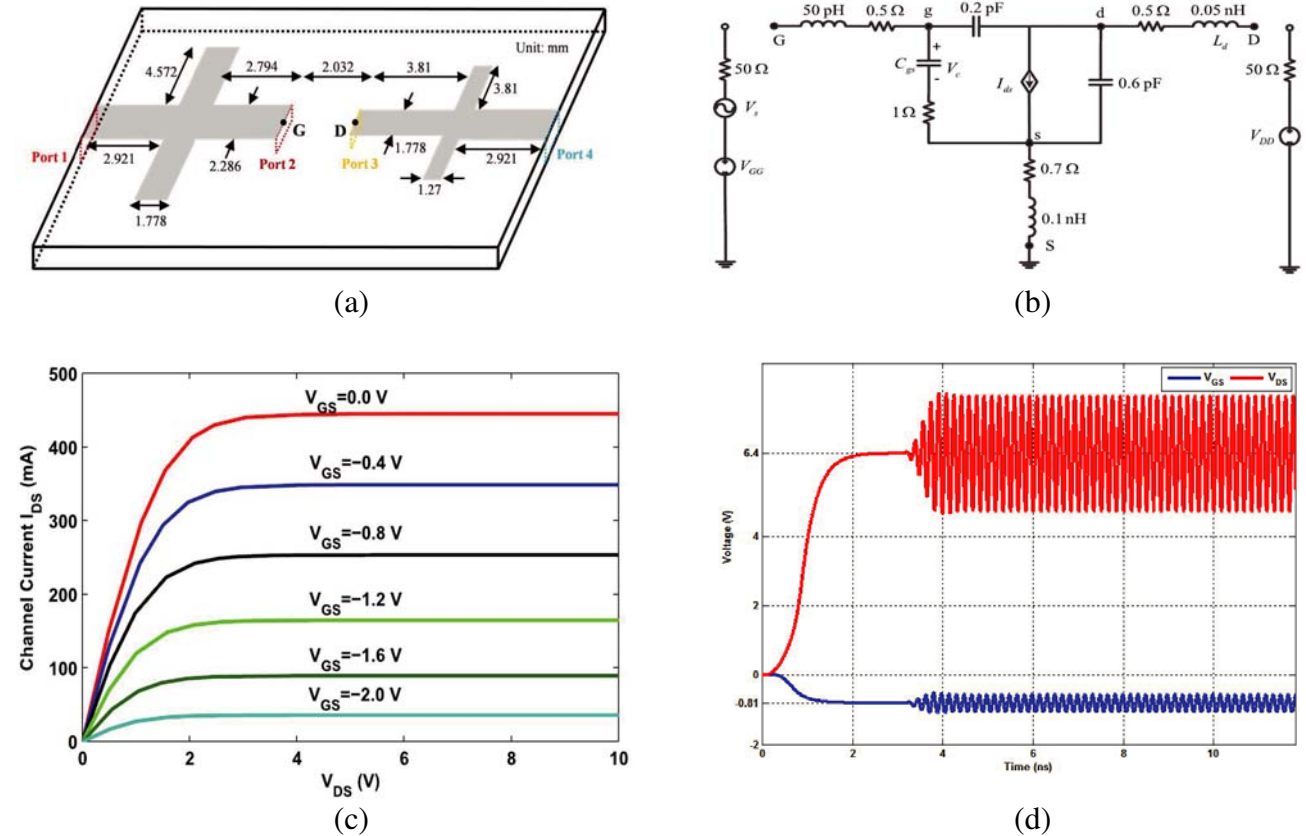
(a)

(b)

(c)

(d)

Figure 2. Electromagnetic-circuital co-simulation of MESFET microwave power amplifier: (a) matching networks, (b) equivalent circuit model, (c) basic current and voltage characteristics of this MESFET amplifier, (d) voltages at the gate and drain terminals obtained from the transient analysis. Reprinted with permission from [36].

methods have been coupled with SBF macromodel for this kind of problem [23, 41–45]. An example of this case is presented in Fig. 4. The nonlinear load is an inverter in ADS using the MOSFET model. The ADS transient simulation is carried out firstly. Then, the currents and voltages at the digital I/O port are recorded as the training data for the SBF macromodel. After that, the SBF macromodel is coupled with DGTD method to implement electromagnetic-circuital co-simulation.

2.2. Electromagnetic-Thermal Co-Simulation Method

The electromagnetic-thermal co-simulation is mainly constituted by electromagnetic simulation and thermal simulation. Maxwell equation is solved to obtain the distribution of electromagnetic field in the electromagnetic simulation. Then, the electromagnetic losses can be computed with the consideration of material loss. After that, heat conduction equation is solved to acquire the thermal field in the thermal simulation. In some cases, the thermal field will influence the electromagnetic properties (constitutive parameters), resulting in the change of electromagnetic fields. Thus a new round of electromagnetic simulation will be needed until a self-consistent solution is reached.

The numerical solution methods and applications of electromagnetic-thermal co-simulation have been studied. At first, microwave heating process is intensively studied by using the FDTD method [46–48]. The influence of the thermal field on the material attributes is considered in [46], and that of frequency-dependent and temperature-dependent media is considered in [47]. Most models consider only heat transfer by conduction, while radiation is usually neglected. This simplification becomes questionable at higher temperatures. Consequently, heat radiation effect is specifically studied in [48].
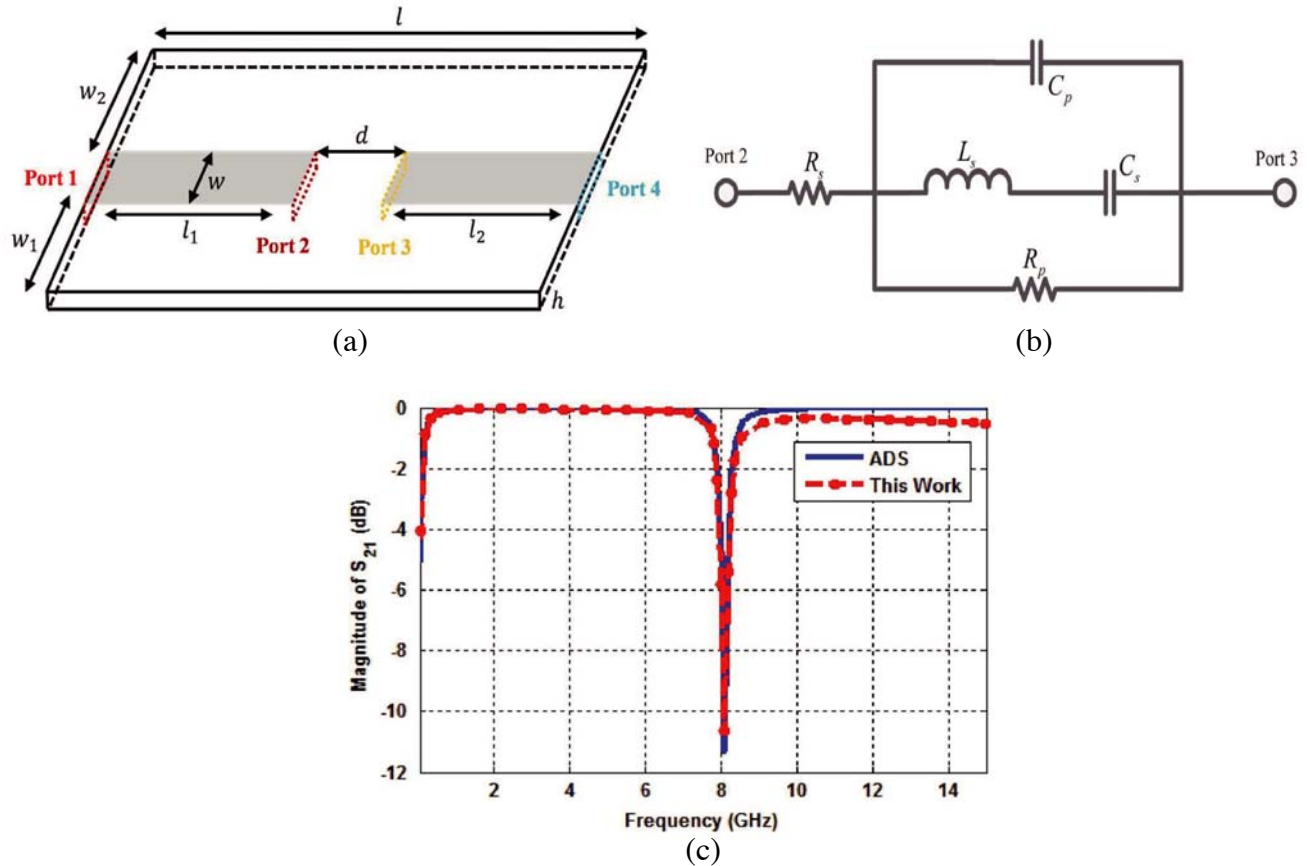
Figure 3. Electromagnetic-circuital co-simulation of a chip capacitor: (a) layout of the circuit configuration, (b) equivalent circuit of the chip capacitor, (c) magnitude of S_{21} calculated by the proposed algorithm and reference from ADS simulation. Reprinted with permission from [37].

Later, owing to the advantage of FEM method in modeling complex geometries and materials, the electromagnetic-thermal co-simulation of integrated circuits and microwave components is carried out based on the FEM method [49–54]. The co-simulation is employed for high-frequency characterizations of the through-silicon-via (TSV) structures in [49] with equivalent circuit models. In [50], electrical-thermal co-simulation is developed to analyze the static voltage drops with the FEM. The effects of the thermal influence and the electrical behaviors of the TSV structures are considered in [51]. The capability of the co-simulation is extended to solve large-scale problems by incorporating a domain decomposition scheme called the finite element tearing and interconnecting (FETI) in [52]. In addition, electrothermal characteristics of some novel 3-D carbon-based heterogeneous interconnects are investigated in [53]. The electrical-thermal co-simulation for high-power microwave components is carried out in [54]. The influence of electromagnetic radiation on human body and the thermal cooling mechanisms of human are investigated in [55–58]. As depicted in Fig. 5, FEM method is adopted for the electromagnetic-thermal co-simulation of human head model exposed to the electromagnetic radiation of cell phones. Due to the advantages of DGTD method over FEM method, recently the DGTD method is also utilized as an efficient numerical method for electromagnetic-thermal co-simulation [59–61]. Transient thermal analysis of 3-D integrated circuits packages is studied in [59]. Transient electromagnetic-thermal co-simulation of a waveguide with filling dielectric is implemented in [60]. Both the frequency-dependent and temperature-dependent properties of dispersive media are considered in [61].
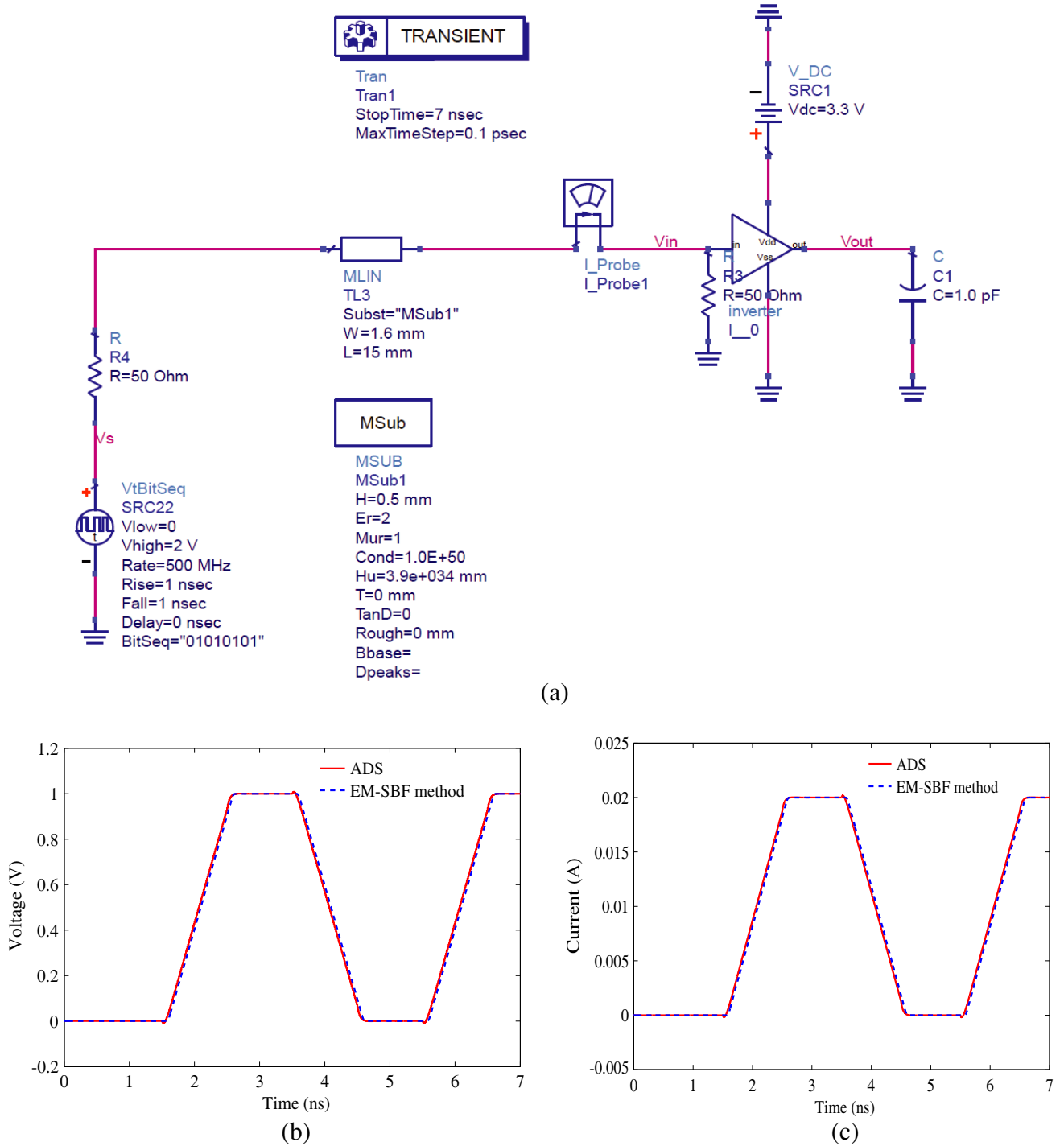
(a)

(b)

(c)

Figure 4. Electromagnetic-circuital co-simulation of digital circuits: (a) the ADS schematic diagram for a microtrip structure loaded with digital circuits, (b) port voltage, (c) port current. Reprinted with permission from [41].

3. THEORY

In this section, we will introduce some basic theories of electromagnetic-circuital-thermal multiphysics simulation including governing equations, numerical methods, coupling mechanisms, etc. Our aim is
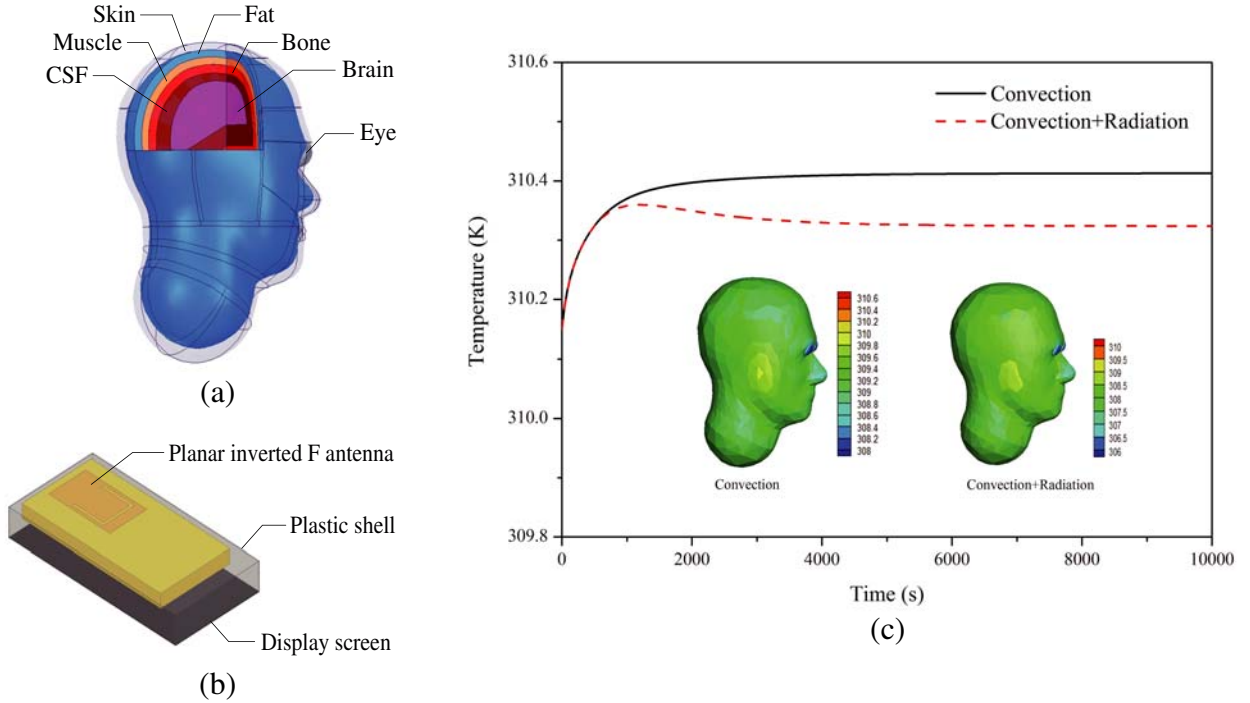
Figure 5. Example of electromagnetic-thermal co-simulation: (a) human head model, (b) cell phone model, (c) the 3D temperature distributions and the temporal temperatures at a randomly chosen observation point. Reprinted with permission from [55].

not to expatiate the related techniques, but to demonstrate the procedures of electromagnetic-circuital-thermal multiphysics simulation.

3.1. Electromagnetic Equations

Let's start from the Maxwell curl equations

$$\nabla \times \mathbf{E} = -\mu \frac{\partial \mathbf{H}}{\partial t} \tag{1}$$

$$\nabla \times \mathbf{H} = \varepsilon \frac{\partial \mathbf{E}}{\partial t} + \sigma \mathbf{E} \tag{2}$$

where μ is the permeability, ε the permittivity, and σ the conductivity. We will describe how to use DGTD method to solve the above two equations.

Suppose that the whole computational domain V can be meshed into a set of tetrahedron elements V_i ($i = 1, ..., N$), whose boundary is ∂V_i. The electric field $\mathbf{E}$ and magnetic field $\mathbf{H}$ in V_i are expanded by a set of vector basis functions $\mathbf{N}_l$. Then, by using the Galerkin testing procedure to the Maxwell curl equations (Galerkin testing means that the testing basis functions $\mathbf{N}_k$ are the same as the expanded basis functions [2].), we can obtain

$$\int_V \mu \mathbf{N}_k \cdot \frac{\partial \mathbf{H}}{\partial t} dV = -\int_V \nabla \times \mathbf{N}_k \cdot \mathbf{E} dV - \int_{\partial V_i} \mathbf{N}_k \cdot \hat{n} \times \mathbf{E} dS \tag{3}$$

$$\int_V \varepsilon \mathbf{N}_k \cdot \frac{\partial \mathbf{E}}{\partial t} dV + \int_V \mathbf{N}_k \cdot \sigma \mathbf{E} dV = \int_V \nabla \times \mathbf{N}_k \cdot \mathbf{H} dV + \int_{\partial V_i} \mathbf{N}_k \cdot \hat{n} \times \mathbf{H} dS \tag{4}$$

The last terms of Eqs. (3) and (4) are evaluated by enforcing the continuity of the numerical flux across element interfaces. There are three most commonly used numerical fluxes, namely the centered

flux, upwind flux, and partially penalized flux. Here we only exhibit the upwind flux:

$$\hat{n} \times \mathbf{E} = \hat{n} \times \frac{Y^i \mathbf{E}^i + Y^j \mathbf{E}^j - \hat{n} \times \mathbf{H}^i + \hat{n} \times \mathbf{H}^j}{Y^i + Y^j} \tag{5}$$

$$\hat{n} \times \mathbf{H} = \hat{n} \times \frac{Z^i \mathbf{H}^i + Z^j \mathbf{H}^j + \hat{n} \times \mathbf{E}^i - \hat{n} \times \mathbf{E}^j}{Z^i + Z^j} \tag{6}$$

where the superscripts i and j refer to the local and neighboring elements, respectively. After plugging Eqs. (5), (6) into Eqs. (3), (4), and expand the electric field $\mathbf{E}^i$ and magnetic field $\mathbf{H}^i$ with $\mathbf{N}_l$, we can write the semi-discretized matrix equation:

$$[M_{hh}^{ii}] \cdot \frac{\partial \mathbf{h}^i}{\partial t} = -[S_{he}^{ii}] \cdot \mathbf{e}^i - [F_{he}^{ii}] \cdot \mathbf{e}^i + [F_{hh}^{ii}] \cdot \mathbf{h}^i - [F_{he}^{ij}] \cdot \mathbf{e}^j - [F_{hh}^{ij}] \cdot \mathbf{h}^j \tag{7}$$

$$[M_{ee}^{ii}] \cdot \frac{\partial \mathbf{e}^i}{\partial t} = [S_{eh}^{ii}] \cdot \mathbf{h}^i + [F_{eh}^{ii}] \cdot \mathbf{h}^i + [F_{ee}^{ii}] \cdot \mathbf{e}^i + [F_{eh}^{ij}] \cdot \mathbf{h}^j - [F_{ee}^{ij}] \cdot \mathbf{e}^j + [C_{ee}^{ii}] \cdot \mathbf{e}^i \tag{8}$$

where

$$[M_{hh}^{ii}] = \int_{V_i} \mu^i \mathbf{N}_k^i \cdot \mathbf{N}_l^i dV \tag{9}$$

$$[M_{ee}^{ii}] = \int_{V_i} \varepsilon^i \mathbf{N}_k^i \cdot \mathbf{N}_l^i dV \tag{10}$$

$$[S_{eh}^{ii}] = \int_{V_i} \nabla \times \mathbf{N}_k^i \cdot \mathbf{N}_l^i dV \tag{11}$$

$$[S_{he}^{ii}] = \int_{V_i} \nabla \times \mathbf{N}_k^i \cdot \mathbf{N}_l^i dV \tag{12}$$

$$[F_{he}^{ii}] = \int_{\partial V_i} \frac{Y^i}{Y^i + Y^j} \mathbf{N}_k^i \cdot \hat{n} \times \mathbf{N}_l^i dS \tag{13}$$

$$[F_{eh}^{ii}] = \int_{\partial V_i} \frac{Z^i}{Z^i + Z^j} \mathbf{N}_k^i \cdot \hat{n} \times \mathbf{N}_l^i dS \tag{14}$$

$$[F_{hh}^{ii}] = \int_{\partial V_i} \frac{1}{Y^i + Y^j} \mathbf{N}_k^i \cdot \hat{n} \times (\hat{n} \times \mathbf{N}_l^i) dS \tag{15}$$

$$[F_{ee}^{ii}] = \int_{\partial V_i} \frac{1}{Z^i + Z^j} \mathbf{N}_k^i \cdot \hat{n} \times (\hat{n} \times \mathbf{N}_l^i) dS \tag{16}$$

$$[F_{he}^{ij}] = \int_{\partial V_i} \frac{Y^j}{Y^i + Y^j} \mathbf{N}_k^i \cdot \hat{n} \times \mathbf{N}_l^j dS \tag{17}$$

$$[F_{eh}^{ij}] = \int_{\partial V_i} \frac{Z^j}{Z^i + Z^j} \mathbf{N}_k^i \cdot \hat{n} \times \mathbf{N}_l^j dS \tag{18}$$

$$[F_{hh}^{ij}] = \int_{\partial V_i} \frac{1}{Y^i + Y^j} \mathbf{N}_k^i \cdot \hat{n} \times (\hat{n} \times \mathbf{N}_l^j) dS \tag{19}$$

$$[F_{ee}^{ij}] = \int_{\partial V_i} \frac{1}{Z^i + Z^j} \mathbf{N}_k^i \cdot \hat{n} \times (\hat{n} \times \mathbf{N}_l^j) dS \tag{20}$$

$$[C_{ee}^{ii}] = -\int_{V_i} \sigma^i \mathbf{N}_k^i \cdot \mathbf{N}_l^i dV \tag{21}$$

By using the leapfrog time integration scheme, the final marching-on-in-time matrix equation of DGTD can be obtained:

$$[M_{hh}^{ii}] \cdot \mathbf{h}_{n+\frac{1}{2}}^i = [M_{hh}^{ii}] \cdot \mathbf{h}_{n-\frac{1}{2}}^i - \Delta t([S_{he}^{ii}] + [F_{he}^{ii}]) \cdot \mathbf{e}_n^i$$
$$+ \Delta t[F_{hh}^{ii}] \cdot \mathbf{h}_{n-\frac{1}{2}}^i - \Delta t[F_{he}^{ij}] \cdot \mathbf{e}_n^j - \Delta t[F_{hh}^{ij}] \cdot \mathbf{h}_{n-\frac{1}{2}}^j \tag{22}$$

$$[M_{ee}^{ii}] \cdot \mathbf{e}_{n+1}^i = [M_{ee}^{ii}] \cdot \mathbf{e}_n^i + \Delta t([S_{eh}^{ii}] + [F_{eh}^{ii}]) \cdot \mathbf{h}_{n+\frac{1}{2}}^i$$
$$+ \Delta t[F_{ee}^{ii}] \cdot \mathbf{e}_n^i + \Delta t[F_{eh}^{ij}] \cdot \mathbf{h}_{n+\frac{1}{2}}^j - \Delta t[F_{ee}^{ij}] \cdot \mathbf{e}_n^j + \Delta t[C_{ee}^{ii}] \cdot \mathbf{e}_n^i \tag{23}$$

3.2. Circuit Equations

The circuit equations constructed for the four types of lumped circuits introduced in Section 2.1 can be summarized into a unified form:

$$\mathbf{I}_n = f(\mathbf{V}_n) \tag{24}$$

where $\mathbf{I}_n$ and $\mathbf{V}_n$ refer to the vectors of node currents and node voltages. This equation can be either linear or nonlinear according to the linear or nonlinear property of the lumped circuits.

3.3. Thermal Equations

The governing equation for transient thermal analysis is heat transfer equation

$$\rho C_\rho \frac{\partial T}{\partial t} = \nabla \cdot (\kappa \nabla T) + Q \tag{25}$$

where ρ denotes the density of the material, κ the thermal conductivity, C_ρ the specific heat coefficient, and Q the heat source.

There are four kinds of commonly-used boundary conditions in thermal analysis [62–64]. For the convenience of description, the surface of an arbitrarily shaped object is denoted by $S = S_0 \cup S_1 \cup S_2 \cup S_3$. If S_0 is maintained at a fixed temperature T_s, the Dirichlet boundary condition will be applied

$$T = T_s \quad r \in S_0 \tag{26}$$

The second category of boundary condition is termed as the Neumann condition, corresponding to a fixed heat flux q_s at the surface S_1

$$-\hat{n} \cdot \kappa \nabla T = q_s \quad r \in S_1 \tag{27}$$

where $\hat{n}$ denotes the unit outward normal vector of the boundary surface.

The third category of boundary condition is the convection boundary condition

$$-\hat{n} \cdot \kappa \nabla T = h(T - T_{sur}) \quad r \in S_2 \tag{28}$$

T_{sur} refers to the surrounding temperature. h denotes the convective heat transfer coefficient.

The fourth category of boundary condition, namely radiation boundary condition, will be applied if thermal radiation occurs between the surface S_3 of the medium and its surrounding environment

$$-\hat{n} \cdot \kappa \nabla T = \epsilon_0 \sigma (T^4 - T_{sur}^4) \quad r \in S_3 \tag{29}$$

where σ is the Stefan-Boltzmann constant. ϵ_0 is the emissivity of the medium surface.

If we employ FETD method to solve Eq. (25), nodal basis functions N_j are employed to expand T

$$T = \sum_{j=1}^{N} T_j N_j \tag{30}$$

Then considering four kinds of boundary conditions, we can obtain the spatially discrete form of Equation (25) by using the Galerkin's scheme with testing basis function N_i $(i = 1, 2, ..., N)$

$$[C]\left\{\frac{\partial T}{\partial t}\right\} + [K]\{T\} = \{f(T)\} \tag{31}$$

where

$$[C]_{ij} = \rho C_\rho \int_V N_i N_j dV \tag{32}$$

$$[K]_{ij} = \kappa \int_V \nabla N_i \cdot \nabla N_j dV + h \int_{S_2} N_i N_j dS \tag{33}$$

$$\{f(T)\}_i = \int_V N_i Q dV - \int_{S_1} N_i q_s dS + h \int_{S_2} N_i T_{sur} dS - \epsilon_0 \sigma \int_{S_3} N_i \left(T^4 - T_{sur}^4\right) dS \tag{34}$$

$\{T\}$ refers to the time-dependent expansion coefficients. The Crank-Nicolson scheme can be utilized for the temporal discretization of Eq. (31) to obtain an unconditionally stable system:

$$\left([C] + [K]\frac{\Delta t}{2}\right)\{T_n\} = \left([C] - [K]\frac{\Delta t}{2}\right)\{T_{n-1}\} + \{f(T_n)\}\Delta t \tag{35}$$

3.4. Coupling Mechanism

1) Electromagnetic-Circuit Coupling

The electromagnetic field in EM structure, the voltages and currents in the lumped circuits vary simultaneously in very short-time scale. So the EM simulation and circuit simulation are tightly coupled. At the interface of the EM structure and circuit, the port voltage can be obtained by a line integral of the electric field in one of the interface elements, which represents the effect of the EM structure on the circuit.

$$v_k = -\int \mathbf{E}^i \cdot \hat{L}_k dL \tag{36}$$

where $\hat{L}_k$ is the unit vector from the reference ground to the desired potential points at the k-th port.

In return, the current will flow from the lumped circuit to the EM structure, which stands for the influence of the lumped circuit on the EM structure. It is worth mentioning that the numerical flux needs to be revised in DGTD method when considering the current from the lumped circuit. In this case, Eqs. (5) and (6) will be changed to

$$\hat{n} \times \mathbf{E} = \frac{\hat{n} \times \left(Y^i \mathbf{E}^i + Y^j \mathbf{E}^j\right)}{Y^i + Y^j} - \frac{\hat{n} \times \left[\hat{n} \times \left(\mathbf{H}^i - \mathbf{H}^j\right) + \mathbf{J}_{\text{CKT}}\right]}{Y^i + Y^j} \tag{37}$$

$$\hat{n} \times \mathbf{H} = \frac{\hat{n} \times \left(Z^i \mathbf{H}^i + Z^j \mathbf{H}^j\right) - Z^j \mathbf{J}_{\text{CKT}}}{Z^i + Z^j} + \frac{\hat{n} \times \left[\hat{n} \times \left(\mathbf{E}^i - \mathbf{E}^j\right)\right]}{Z^i + Z^j} \tag{38}$$

where $\mathbf{J}_{\text{CKT}}$ denotes the surface current density injected by the lumped circuit at the interface of EM structure and circuit. Fig. 6(a) shows the pseudocodes of electromagnetic-circuit co-simulation. A detailed implementation of the electromagnetic-circuit coupling can be found [37, 41].

2) Electromagnetic-Thermal Coupling

As shown in Fig. 7, there are two coupling schemes of electromagnetic and thermal co-simulation, namely one-way coupling scheme and two-way coupling scheme. For the one-way coupling scheme, the dissipated power calculated through EM simulation becomes the heat source in the thermal simulation. For example, the dissipated power due to conductor loss can be calculated as

$$P_d = \sigma|\mathbf{E}|^2 \tag{39}$$

The distribution of electromagnetic field will influence the temperature of objects, but the temperature of objects has no influence on the EM simulation.

```
Initialization:
    port voltage V₀ = 0, port current I₀ = 0,
    electric field e₀ = 0, magnetic field h₀ = 0
For n=1 to number of time steps
    For i=1 to number of elements
        If current element is connected with lumped circuit
            Solve the coupled EM-circuit equation
        else
            Solve the EM matrix equations
        endif
    End Loop i
End Loop n
Output: electric field eₙ, magnetic field hₙ, port current
Iₙ, port voltage Vₙ.
```

```
Initialization:
    temperature T₀ = T,
    electric field e₀ = 0,
    magnetic field h₀ = 0,
    conductivity σ = σ₀.
For n=1 to number of time steps
    Compute electromagnetic field eₙ and hₙ
    Calculate dissipated power P_d
    Compute temperature Tₙ with Q = P_d
    Update conductivity σ
End Loop n
Output: electric field eₙ, magnetic field hₙ,
temperature Tₙ.
```

(a)   (b)

Figure 6. Pseudocodes of (a) electromagnetic-circuit co-simulation, (b) electromagnetic-thermal cosimulation.

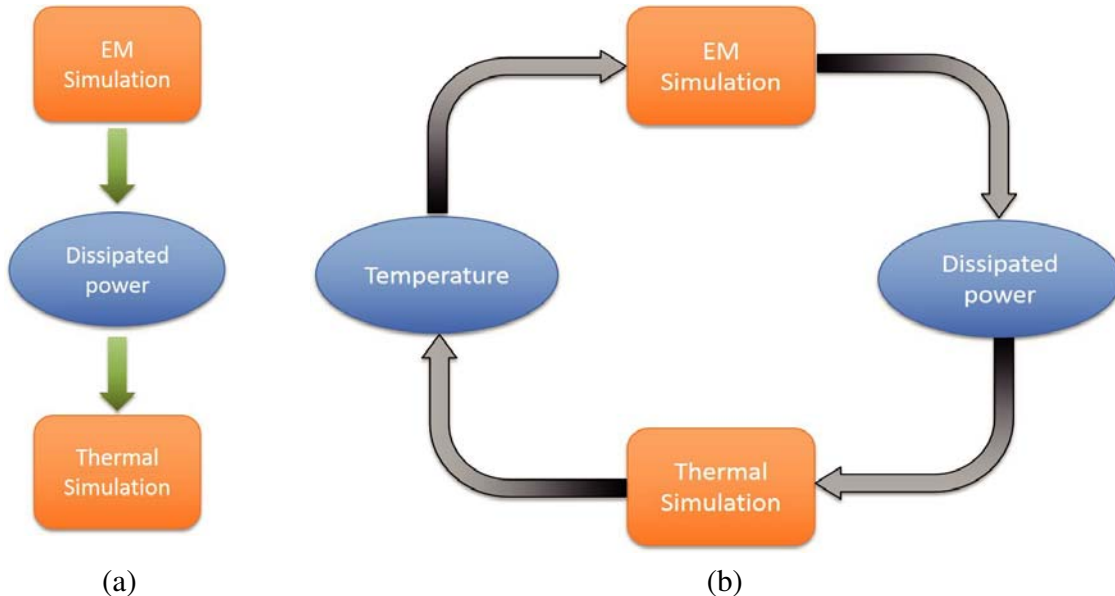(a)   (b)

Figure 7. Coupling schemes of electromagnetic and thermal co-simulation: (a) one-way coupling scheme, (b) two-way coupling scheme.

In the two-way coupling scheme, the EM and thermal simulations are coupled in an iterative manner. After considering the influence of EM to thermal, the variation of temperature of objects will cause the change of permittivity, conductivity, etc., which will in turn affect the electromagnetic simulation. For instance, the electrical conductivity can be the function of temperature

$$\sigma = g(T) \tag{40}$$

Figure 6(b) shows the pseudocodes of electromagnetic-thermal co-simulation.

4. CONCLUSION

In this paper, we have reviewed the state of the art of the electromagnetic-circuital-thermal multiphysics simulation method. Apparently, a great number of works have been done on electromagnetic-circuital co-simulation and electromagnetic-thermal co-simulation. However, the simultaneous simulation of all three, namely electromagnetic, circuit, and thermal, has not been found yet. Actually, we have completed this work quite recently. The technical details will be shown in another paper. Also, we think the application of the electromagnetic-circuital-thermal multiphysics simulation to real engineering problems is another challenging and urgent task in future.

ACKNOWLEDGMENT

REFERENCES

1. Yee, K. S., "Numerical solution of initial boundary value problems involving Maxwell's equations in isotropic media," *IEEE Trans. Antennas Propag.*, Vol. 14, No. 3, 302–307, May 1966.

2. Jin, J. M., *The Finite Element Method in Electromagnetics*, 2nd Edition, John Wiley & Sons, Inc., New York, 2002.

3. Harrington, R. F., *Field Computation by Moment Methods*, The Macmullan Company, 1968.

4. Huang, C. C. and T. H. Chu, "Analysis of wire scatterers with nonlinear or time-harmonic loads in the frequency domain," *IEEE Trans. Antennas Propag.*, Vol. 41, No. 1, 25–30, Jan. 1993.

5. Dault, D., B. Shanker, A. D. Baczewski, and P. Chahal, "Modeling of dense coupled periodic and non-periodic electromagnetic-circuit systems using harmonic balance and fast solvers," *Proc. USNC/URSI Rad. Sci. Meeting*, Jul. 2011.

6. Lee, J. F., R. Lee, and A. Cangellaris, "Time-domain finite element methods," *IEEE Trans. Antennas Propag.*, Vol. 45, No. 3, 430–442, Mar. 1997.

7. Zhang, H. H., Z. H. Fan, and R. S. Chen, "Marching-on-in-degree solver of time-domain finite element-boundary integral method for transient electromagnetic analysis," *IEEE Trans. Antennas Propag.*, Vol. 62, No. 1, 319–326, Jan. 2014.

8. Shanker, B., M. Lu, J. Yuan, and E. Michielssen, "Time domain integral equation analysis of scattering from composite bodies via exact evaluation of radiation fields," *IEEE Trans. Antennas Propag.*, Vol. 57, No. 5, 1506–1520, May 2009.

9. Zhang, H. H., Q. Q. Wang, Y. F. Shi, and R. S. Chen, "Efficient marching-on-in-degree solver of time domain integral equation with adaptive cross approximation algorithm-singular value decomposition," *Appl. Comput. Electromagn. Soc. J.*, Vol. 27, No. 6, 475–482, Jun. 2012.

10. Ding, D. Z., H. H. Zhang, and R. S. Chen, "Marching-on-in-degree method with delayed weighted Laguerre polynomials for transient electromagnetic scattering analysis," *IEEE Trans. Antennas Propag.*, Vol. 63, No. 4, 1822–1827, Apr. 2015.

11. He, Z., H. H. Zhang, and R. S. Chen, "Parallel marching-on-in-degree solver of time-domain combined field integral equation for bodies of revolution accelerated by MLACA," *IEEE Trans. Antennas Propag.*, Vol. 63, No. 8, 3705–3710, Aug. 2015.

12. Kuo, C. N., B. Houshmand, and T. Itoh, "Full-wave analysis of packaged microwave circuits with active and nonlinear devices: An FDTD approach," *IEEE Trans. Microw. Theory Tech.*, Vol. 45, No. 5, 819–826, Aug. 2015.

13. Pereda, J. A., F. Alimenti, P. Mezzanotte, L. Roselli, and R. Sorrentino, "A new algorithm for the incorporation of arbitrary linear lumped networks into FDTD simulators," *IEEE Trans. Microw. Theory Tech.*, Vol. 47, No. 6, 943–949, Jun. 1999.

14. Wu, T. L., S. T. Chen, and Y. S. Huang, "A novel approach for the incorporation of arbitrary linear lumped network into FDTD method," *IEEE Microw. Wireless Compon. Lett.*, Vol. 14, No. 2, 74–76, Feb. 2004.

15. Gonzalez, O., J. A. Pereda, A. Herrera, and A. Vegas, "An extension of the lumped-network FDTD method to linear two-port lumped circuits," *IEEE Trans. Microw. Theory Tech.*, Vol. 54, No. 7, 3045–3051, Jul. 2006.

16. Ma, K. P., M. Vhen, B. Houshband, Y. Qian, and T. Itoh, "Global time-domain full-wave analysis of microwave circuits involving highly nonlinear phenomena and EMC effects," *IEEE Trans. Microw. Theory Tech.*, Vol. 47, No. 6, 859–866, Jun. 1999.

17. Wang, C. C. and C. W. Kuo, "An efficient scheme for processing arbitrary lumped multiport devices in the finite-difference time-domain method," *IEEE Trans. Microw. Theory Tech.*, Vol. 55, No. 5, 958–965, May 2007.

18. Tsai, H. P., Y. Wang, and T. Itoh, "An unconditionally stable extended (USE) finite-element time-domain solution of active nonlinear microwave circuits using perfectly matched layers," *IEEE Trans. Microw. Theory Tech.*, Vol. 50, No. 10, 2226–2232, Oct. 2002.

19. He, Q. and D. Jiao, "Fast electromagnetic-based co-simulation of linear network and nonlinear circuits for the analysis of high-speed integrated circuits," *IEEE Trans. Microw. Theory Tech.*, Vol. 58, No. 12, 3677–3687, Dec. 2010.

20. Wang, R. and J. M. Jin, "Incorporation of multiport lumped networks into the hybrid time-domain finite-element analysis," *IEEE Trans. Microw. Theory Tech.*, Vol. 57, No. 8, 2030–2037, Aug. 2009.

21. Yang, C. Y. and V. Jandhyala, "Time domain surface integral technique for mixed EM and circuit simulation," *IEEE. Trans. Adv. Pack.*, Vol. 28, No. 4, 745–753, Nov. 2005.

22. Ayg, K., B. C. Fischer, J. Meng, B. Shanker, and E. Michielssen, "A fast hybrid field-circuit simulator for transient analysis of microwave circuits," *IEEE Trans. Microw. Theory Tech.*, Vol. 52, No. 2, 573–583, Feb. 2004.

23. Zhang, H. H., L. J. Jiang, and H. M. Yao, "Embedding the behavior macromodel into TDIE for transient field-circuit simulations," *IEEE Trans. Antennas Propag.*, Vol. 64, No. 7, 3233–3238, Jul. 2016.

24. Yilmaz, A. E., J. M. Jin, and E. Michielssen, "A parallel FFT accelerated transient field-circuit simulator," *IEEE Trans. Microw. Theory Tech.*, Vol. 53, No. 9, 2851–2865, Sep. 2005.

25. Chen, S. T., D. Z. Ding, Z. H. Fan, and R. S. Chen, "Nonlinear analysis of microwave limiter using field-circuit coupling algorithm based on time-domain volume-surface integral method," *IEEE Microw. and Wireless Compon. Lett.*, Vol. 27, No. 10, 864–866, Oct. 2017.

26. Chen, S., D. Ding, R. Chen, and R. Chen, "A hybrid volume-surface integral spectral-element time-domain method for nonlinear analysis of microwave circuit," *IEEE Antennas and Wireless Propag. Lett.*, Vol. 16, 3034–3037, 2017.

27. Chen, S., D. Ding, and R. Chen, "Time-domain impulse response with the TD-VSIE field-circuit coupling algorithm for nonlinear analysis of microwave amplifier," *IEEE Microw. and Wireless Compon. Lett.*, Vol. 28, No. 5, 431–433, May 2018.

28. Lu, T., P. Zhang, and W. Cai, "Discontinuous Galerkin methods for dispersive and lossy Maxwell's equations and PML boundary conditions," *Journal of Computational Physics*, Vol. 200, No. 2, 549–580, Nov. 2004.

29. Chen, G., L. Zhao, W. Yu, and J. Jin, "Discontinuous Galerkin time-domain method for devices with lumped elements," *2017 International Applied Computational Electromagnetics Society Symposium (ACES)*, 1–2, Suzhou, 2017.

30. Chen, J. and Q. H. Liu, "Discontinuous Galerkin time-domain methods for multiscale electromagnetic simulations: A review," *Proceedings of the IEEE*, Vol. 101, No. 2, 242–254, Feb. 2013.

31. Yan, S. and J. Jin, "A DGTD-based multiscale simulator for electromagnetic multiphysics problems," *2019 IEEE International Symposium on Antennas and Propagation and USNC-URSI Radio Science Meeting*, 1057–1058, Atlanta, GA, USA, 2019.

32. Yan, S., J. Qian, and J. Jin, "An adaptive discontinuous Galerkin time-domain method for multiphysics and multiscale simulations," *2019 International Conference on Electromagnetics in Advanced Applications (ICEAA)*, 0592-0592, Granada, Spain, 2019.

33. Ho, C. W., A. E. Ruehli, and P. A. Brennan, "The modified nodal approach to network analysis," *IEEE Trans. Circuits Syst.*, Vol. 22, No. 6, 504–509, Jun. 1975.

34. Press, W. H., S. A. Teukolsky, W. T. Vetterling, and B. P. Flannery, *Numerical Recipes in Fortran*, Cambridge Univ. Press, New York, 1992.

35. Dosopoulos, S. and J. F. Lee, "Interconnect and lumped elements modeling in interior penalty discontinuous Galerkin time-domain methods," *J. Comput. Phys.*, Vol. 229, 8521–8536, Aug. 2010.

36. Li, P., L. J. Jiang, and H. Bagci, "Co-simulation of electromagnetics-circuit systems exploiting DGTD and MNA," *IEEE Trans. Compon., Packag. Manuf. Tech.*, Vol. 4, No. 6, 1052–1061, Jun. 2014.

37. Li, P. and L. J. Jiang, "Integration of arbitrary lumped multiport circuit networks into the discontinuous Galerkin time-domain analysis," *IEEE Trans. Microw. Theory Tech.*, Vol. 61, No. 7, 2525–2534, Jul. 2013.

38. Scott, I., V. Kumar, C. Christopoulos, D. W. P. Thomas, S. Greedy, and P. Sewell, "Integration of behavioral models in the full-field TLM method," *IEEE Trans. Electromagn. Compat.*, Vol. 54, No. 2, 359–366, Feb. 2003.

39. Grivet-Talocia, S., I. S. Stievano, and F. G. Canavero, "Hybridization of FDTD and device behavioral-modeling techniques [interconnected digital I/O ports]," *IEEE Trans. Electromagn. Compat.*, Vol. 45, No. 1, 31–42, Apr. 2012.

40. Stievano, I. S., I. A. Maio, and P. Sewell, "Mπlog, macromodeling via parametric identification of logic gates," *IEEE Trans. Adv. Packag.*, Vol. 27, No. 1, 15–23, Feb. 2004.

41. Zhang, H. H., L. J. Jiang, H. M. Yao, and Y. Zhang, "Transient heterogeneous electromagnetic simulation with DGTD and behavioral macromodel," *IEEE Trans. Electromagn. Compat.*, Vol. 59, No. 4, 1152–1160, Aug. 2017.

42. Yuan, P., H. H. Zhang, L. J. Jiang, D. G. Donoro, and Y. Zhang, "Electromagnetic-circuit cosimulation based on hybrid explicit-implicit DGTD and SBF macromodel," *The IEEE Electrical Design of Advanced Packaging and Systems (EDAPS) Symposium*, Haining, China, Dec. 2017.

43. Zhang, H. H., L. J. Jiang, H. M. Yao, and Y. Zhang, "Coupling DGTD and behavioral macromodel for transient heterogeneous electromagnetic simulations," *2016 IEEE International Symposium on Electromagnetic Compatibility*, Ottawa, Canada, Jul. 2016.

44. Zhang, H. H., H. M. Yao, and L. J. Jiang, "Novel time domain integral equation method hybridized with the macromodels of circuits," *The 24th Conference on Electrical Performance of Electronic Packages and Systems (EPEPS)*, San Jose, CA, USA, Oct. 2015.

45. Yao, H. M., L. J. Jiang, H. H. Zhang, and W. E. I. Sha, "Machine learning methodology review for computational electromagnetics," *2019 International Applied Computational Electromagnetics Society (ACES) Symposium in China*, Beijing, China, Aug. 2019.

46. Ma, L. and D. L. Paul, "Experimental validation of a combined electromagnetic and thermal FDTD model of a microwave heating process," *IEEE Trans. Microw. Theory Tech.*, Vol. 1, No. 43, 2565–2572, 1995.

47. Torres, F. and B. Jecko, "Complete FDTD analysis of microwave heating processes in frequency-dependent and temperature-dependent media," *IEEE Trans. Microw. Theory Tech.*, Vol. 45, No. 1, 108–117, 1997.

48. Haala, J. and W. Wiesbeck, "Modeling microwave and hybrid heating processes including heat radiation effects," *IEEE Trans. Electromagn. Compat.*, Vol. 50, No. 5, 1346–1354, 2002.

49. Liu, E., E. Li, W. Ewe, and H. M. Lee, "Multi-physics modeling of through-Silicon vias with equivalent-circuit approach," *19th Topical Meeting on Electrical Performance of Electronic*

Packaging and Systems (EPEPS), 33–36, Austin, TX, 2010.

50. Lu, T. and J. M. Jin, "Electrical-thermal co-simulation for DCIR-drop analysis of large-scale power delivery," *IEEE Trans. Compon., Packag. Manuf. Tech.*, Vol. 4, No. 2, 323–331, Feb. 2014.

51. Lu, T. and J. M. Jin, "Thermal-aware high-frequency characterization of large-scale through-Silicon-via structures," *IEEE Trans. Compon., Packag. Manuf. Tech.*, Vol. 4, No. 6, 1015–1025, 2014.

52. Lu, T. J. and J. M. Jin, "Transient electrical-thermal analysis of 3-D power distribution network with FETI-enabled parallel computing," *IEEE Trans. Compon., Packag. Manuf. Tech.*, Vol. 4, No. 10, 1684–1695, 2014.

53. Li, N., J. F. Mao, W. S. Zhao, M. Tang, W. C. Chen, and W. Y. Yin, "Electrothermal cosimulation of 3-D carbon-based heterogeneous interconnects," *IEEE Trans. Compon., Packag. Manuf. Tech.*, Vol. 6, No. 4, 1–9, 2016.

54. Lu, T. J. and J. M. Jin, "Electrical-thermal co-simulation for analysis of high-power RF/microwave components," *IEEE Trans. Electromagn. Compat.*, Vol. 59, No. 1, 93–102, 2017.

55. Zhang, H. H., W. E. I. Sha, et al., "Electromagnetic-thermal analysis of human head exposed to cell phones with the consideration of radiative cooling," *IEEE Antennas and Wireless Propag. Lett.*, Vol. 17, No. 9, 1584–1587, Jul. 2018.

56. Zhang, H. H., Y. Liu, X. Y. Z. Xiong, G. M. Shi, C. Y. Wang, and W. E. I. Sha, "Investigating thermal cooling mechanisms of human body under exposure to electromagnetic radiation," *IEEE Access*, Vol. 7, 9697–9703, 2019.

57. Chen, P. Y., H. H. Zhang, G. G. Yu, W. E. I. Sha, C. Y. Wang, and Y. Y. An, "Cooling mechanisms of human under high-power electromagnetic radiation," *2019 IEEE International Conference on Computational Electromagnetics (ICCEM)*, Shanghai, China, Mar. 2019.

58. Zhang, H. H., P. Yuan, P. Y. Chen, and W. W. Choi, "Simulation of temperature increase of human head model exposed to cell phones," *2018 International Applied Computational Electromagnetics Society (ACES) Symposium in China*, Beijing, China, Jul. 2018.

59. Li, P., Y. Dong, M. Tang, et al., "Transient thermal analysis of 3-D integrated circuits packages by the DGTD method," *IEEE Trans. Compon., Packag. Manuf. Tech.*, 1–10, 2017.

60. Chen, P. Y., H. H. Zhang, E. I. W. Sha, and D. Z. Ding, "Transient electromagnetic-thermal co-simulation based on DGTD method," *2019 International Applied Computational Electromagnetics Society Symposium-China (ACES)*, 1–2, Nanjing, China, 2019.

61. Dong, Y., M. Tang, P. Li, and J. Mao, "Transient electromagnetic-thermal simulation of dispersive media using DGTD method," *IEEE Trans. Electromagn. Compat.*, Vol. 61, No. 4, 1305–1313, 2019.

62. Zhang, H. H., W. E. I. Sha, Z. X. Huang, and G. M. Shi, "Flexible and accurate simulation of radiation cooling with FETD method," *Scientific Reports*, Vol. 8, No. 1, 2652–2661, Feb. 2018.

63. Zhang, H. H., P. Y. Chen, W. E. I. Sha, and Z. X. Huang, "Accurate simulation of convection and radiation cooling for a 3D IC package," *2018 IEEE International Conference on Computational Electromagnetics (ICCEM)*, Chengdu, China, Mar. 2018.

64. Zhang, H. H., W. E. I. Sha, Z. X. Huang, and Y. Zhang, "Simulation of radiative cooling with FETD method," *The IEEE Electrical Design of Advanced Packaging and Systems (EDAPS) Symposium*, Haining, China, Dec. 2017.